

Interplay between quantum Zeno and anti-Zeno effects in a non-degenerate hyper-Raman nonlinear optical coupler

Moumita Das,¹ Kishore Thapliyal,^{2,*} Biswajit Sen,^{3,†} Jan Peřina,⁴ and Anirban Pathak^{5,‡}

¹*Department of Physics, Siliguri College, Siliguri - 734 001, India*

²*RCPTM, Joint Laboratory of Optics of Palacky University and Institute of Physics of Academy of Science of the Czech Republic, Faculty of Science, Palacky University, 17. listopadu 12, 771 46 Olomouc, Czech Republic*

³*Department of Physics, Vidyasagar Teachers' Training College, Midnapore - 721 101, India*

⁴*Joint Laboratory of Optics of Palacky University and Institute of Physics of Academy of Science of the Czech Republic, Faculty of Science, Palacky University, 17. listopadu 12, 771 46 Olomouc, Czech Republic*

⁵*Jaypee Institute of Information Technology, A-10, Sector-62, Noida UP-201309, India*

Quantum Zeno and anti-Zeno effects are studied in an asymmetric nonlinear optical coupler composed of a probe waveguide and a system waveguide. The system is a nonlinear waveguide operating under non-degenerate hyper-Raman process, while both the pump modes in the system are constantly interacting with the probe waveguide. The effect of the presence of probe on the temporal evolution of the system in terms of the number of photons in Stokes and anti-Stokes modes as well as phonon number is quantified as Zeno parameter. The negative (positive) values of the Zeno parameter in the specific mode are considered as the signatures of the quantum Zeno (anti-Zeno) effect in that mode of the system. It is observed that the phase mismatch in Stokes and anti-Stokes generation processes can be controlled to induce a transition between quantum Zeno and anti-Zeno effects for both off-resonant and resonant hyper-Raman process. However, in case of off-resonant hyper-Raman process in the system waveguide, the frequency detuning parameters can also be used analogously to cause the desired crossover. Further, the general nature of the physical system and the perturbative technique used here allowed us to analytically study the possibilities of observing quantum Zeno and anti-Zeno effects in a large number of special cases, including situations where the process is spontaneous, partially spontaneous and/or the system is operated under degenerate hyper-Raman process, or a simple Raman process.

I. INTRODUCTION

The response of a quantum system to a measuring device, cannot only distinctively distinguish a quantum system from a classical system, it also plays an extremely important role in the subsequent evolution of the system. Interestingly, sufficiently frequent interactions can even suppress the time evolution. This phenomenon of suppressing (inhibition of) the time evolution of a quantum system by frequent interaction is known as the quantum Zeno effect (QZE) [1]. It was introduced by Mishra and Sudarshan in 1977[1], in an interesting work, where they showed that if an unstable particle is continuously measured, it will never decay. They realized that this situation is analogous to one of the well-known Zeno's paradoxes which were introduced by the Greek philosopher Zeno of Elea in the 5th century BC and which have persistently fascinated scientists and philosophers since then. Considering the analogy, Mishra and Sudarshan referred to the quantum phenomenon analogous to classical Zeno's paradox as *Zeno's paradox in quantum theory*. This led to the formal origin of QZE, but the quantum analogue of Zeno's paradox was also studied before the work of Mishra and Sudarshan [1]. Specifically, Khalifin had studied nonexponential decay of unstable atoms [2] in the late fifties and early sixties. Interestingly, it was soon recognized that measurement can also lead to a phenomenon which can be viewed as the inverse of QZE. In such a phenomenon, continuous measurement (or in-

teraction) leads to the enhancement of the evolution instead of the inhibition (see Refs. [3–8]) and is referred to as quantum anti-Zeno effect (QAZE) or inverse Zeno effect. Interestingly, QZE and QAZE are known to be evinced through various equivalent ways [9]. For the present work, a particularly relevant manifestation of QZE would be one in which QZE or QAZE is viewed as a process led by continuous interaction between a system and a probe. Specifically, in what follows, we aim to study the continuous interaction-type manifestation of QZE in hyper-Raman processes, where it will be considered that a nonlinear waveguide is operating under non-degenerate hyper-Raman process and is continuously interacting with a probe waveguide. A change in the dynamics of the nonlinear system waveguide due to the presence of the probe waveguide is quantified as increase/decrease in the photon numbers of Stokes and anti-Stokes modes as well as phonon number. Earlier, QZE is reported by some of the present authors in Raman process [10], an asymmetric and a symmetric nonlinear optical couplers [6, 8], and parity-time symmetric linear optical coupler [7]. However, it was never been studied in the systems involving hyper-Raman process due to its intrinsic mathematical difficulty.

Apart from the Raman process, QZE and QAZE has already been studied in various optical systems, like various types of optical couplers [6, 10–13], parametric down-conversion [14–16], parametric down conversion with losses [17], an arrangement of beam splitters [18]. In these studies on QZE in optical systems, often the pump mode has been considered strong, and thus the complexity of a completely quantum mechanical treatment has been circumvented. Keeping this in mind, here we plan to use a completely quantum mechanical description of the nonlinear optical coupler composed of

* kishore.thapliyal@upol.cz

† bsen75@yahoo.co.in

‡ anirban.pathak@jiit.ac.in

a probe and a nonlinear waveguide operating under hyper-Raman process. We have considered a general Raman process here, namely non-degenerate hyper-Raman process, which allows us to reduce the corresponding results for Raman and degenerate hyper-Raman processes.

For about two decades, since the pioneering work of Mishra and Sudarshan, QZE remained as a problem of theoretical interest without any practical applications. The scenario started changing from the beginning of nineties as it became possible to experimentally realize QZE using different routes [19–21]. This enhanced the interest on QZE and that in turn led to many new proposals for applications of QZE [19, 22–25]. For example, applications of QZE were proposed for the enhancement of the resolution of absorption tomography [24, 25], reduction of communication complexity [26], in combating decoherence by confining dynamics in decoherence-free subspace [27]. Further, proposals for quantum interrogation measurement [19] and counterfactual direct quantum communication protocol [23, 28] using QZE have garnered much attention. Efforts have also been made to investigate QZE in the macroscopic world for large black holes [29] and in nonlinear waveguides in the context of stationary flows with localized dissipation [30]. Inspired by these applications of QZE, a general nature of the nonlinear (non-degenerate hyper-Raman) process under consideration, and availability of nonlinear optical couplers in integrated optics and optical fiber [31, 32], here we study the possibility of QZE and QAZE using a completely quantum treatment in an asymmetric nonlinear optical coupler.

Using a perturbative technique (known as Sen-Mandal technique [33–36]) for obtaining an operator solution of Heisenberg’s equations of motion, we have obtained closed form analytic expressions for the spatial evolution of the relevant field operators present in the system momentum operator that provides a completely quantum mechanical description of nonlinear optical coupler composed of the probe and a nonlinear waveguide operating under hyper-Raman process. It is well established that this method produces better results compared to the conventional short-length approach [33–36] as the present solution is not restricted by length/time. In what follows, we will see that the use of this perturbative technique has revealed compact analytic expressions for Zeno parameter which clearly illustrate that in the system under consideration (and in many special cases of it), it is possible to observe QZE and QAZE in Stokes, anti-Stokes, and phonon modes for the suitable choices of system parameters. Further, it will be shown that phase mismatch and frequency detuning parameters can be controlled to execute a crossover between QZE and QAZE.

The rest of the paper is organized as follows. In Section II, we briefly describe the hyper-Raman process based asymmetric nonlinear optical coupler system of our interest. Subsequently, we report the expressions of Zeno parameter for both photon and phonon modes in system in Section III. A detailed discussion of the obtained results is summarized in Section IV. Finally, the paper is concluded in Section V.

II. PHYSICAL SYSTEM

The physical system of our interest is actually a codirectional asymmetric nonlinear optical coupler composed of a probe and a system, which is a nonlinear waveguide operating under hyper-Raman process (see Fig. 1 for a schematic diagram). The momentum operator of the complete (probe+system) physical system is given by

$$G = \omega_p a_p^\dagger a_p + \omega_{a_1} a_1^\dagger a_1 + \omega_{a_2} a_2^\dagger a_2 + \omega_b b^\dagger b + \omega_c c^\dagger c + \omega_d d^\dagger d + \left(g a_1 a_2 b^\dagger c^\dagger + \chi a_1 a_2 c d^\dagger + \Gamma a_p a_1^\dagger a_2^\dagger + \text{H.c.} \right), \quad (1)$$

where $\hbar = 1$ (the same convention is used in the rest of the paper), and H.c. stands for the Hermitian conjugate. The annihilation (creation) operators a_p (a_p^\dagger), a_i (a_i^\dagger), b (b^\dagger), c (c^\dagger), and d (d^\dagger) correspond to the probe pump (indexed by subscript p), non-degenerate hyper-Raman laser (this is also a pump, but it is indexed by subscript $i = 1, 2$ to distinguish from the probe pump), Stokes, vibration (phonon), and anti-Stokes modes, respectively. All field operators introduced here, obey the usual bosonic commutation relation. Frequencies corresponding to the probe, Pump 1 and 2, Stokes, phonon and anti-Stokes modes are denoted by ω_p , ω_{a_1} , ω_{a_2} , ω_b , ω_c , and ω_d , respectively. The Stokes and anti-Stokes coupling constants are described by parameters g and χ , respectively. Further, Γ denotes the interaction constant between the probe and the two pump modes present in the hyper-Raman process in the system. We obtain the Heisenberg’s equations of motion for the momentum operator (1) of the system of interest, which gives us six coupled differential equations for the six bosonic operators present in the expression of the momentum operator. To obtain the spatial evolution of all the operators we use Sen-Mandal perturbative technique as dimensionless quantities gz , χz , and Γz are small compared to unity. In Appendix A, we have reported the analytic operator solution of the Heisenberg’s equations of motion using the Sen-Mandal technique and spatial evolution of the relevant field operators including number operators for Stokes, anti-Stokes, and phonon modes. In the next section, we will show that the obtained number operators would provide us analytic expressions of Zeno parameter for the respective modes. The general nature of the solution and the process under consideration allow us to deduce the results for Raman and degenerate hyper-Raman processes as well as corresponding short-length solution in the limiting cases. Further, the present solution inherently introduces frequency detuning parameters in the Stokes and anti-Stokes generation, and thus provides solutions for both resonant and off-resonant set of Raman processes.

III. QUANTUM ZENO AND ANTI-ZENO EFFECT

In order to investigate the QZE and QAZE in hyper-Raman active medium we consider the initial composite coherent state $|\psi(0)\rangle$ as the product of the initial coherent states of probe, pump, Stokes, phonon and anti-Stokes modes as $|\alpha\rangle$, $|\alpha_j\rangle$, $|\beta\rangle$, $|\gamma\rangle$, and $|\delta\rangle$, respectively. Hence the initial state is

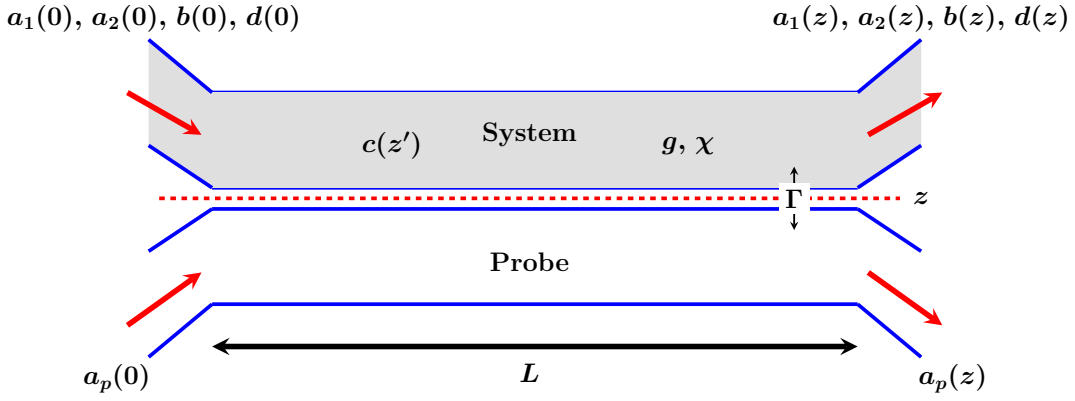


Figure 1. (Color online) Schematic diagram of an optical coupler of length L composed a system waveguide, operating under non-degenerate hyper-Raman process, interacting with a probe. The coupling coefficients as well as optical and phonon modes are indicated in the diagram.

considered to be

$$|\psi(0)\rangle = |\alpha\rangle \otimes |\alpha_1\rangle \otimes |\alpha_2\rangle \otimes |\beta\rangle \otimes |\gamma\rangle \otimes |\delta\rangle, \quad (2)$$

and the field operator a_p operating on the initial state gives

$$a_p(0) |\psi(0)\rangle = \alpha |\alpha\rangle \otimes |\alpha_1\rangle \otimes |\alpha_2\rangle \otimes |\beta\rangle \otimes |\gamma\rangle \otimes |\delta\rangle, \quad (3)$$

where $\alpha = |\alpha| e^{i\varphi_p}$ is the complex eigenvalue with $|\alpha|^2$ mean number of photons and φ_p phase angle in the probe mode a . In the similar manner, coherent state parameters for all the optical and phonon modes involved in the hyper-Raman process can be defined as $\Lambda_j = |\Lambda_j| e^{i\varphi_j}$ for complex amplitudes $\Lambda_j : \Lambda \in \{\alpha, \beta, \gamma, \delta\}$ and corresponding phase angle φ_j with $j \in \{1, 2, b, c, d\}$ for the non-degenerate Pump-1 and Pump-2, Stokes, phonon, and anti-Stokes modes, respectively.

We define the Zeno parameter as [6–8]

$$Z_i = \langle N_i \rangle - \langle N_i \rangle_{\Gamma=0}, \quad (4)$$

where $i \in \{b, c, d\}$ and N is the number operator. The conditions $Z_i < 0$ and $Z_i > 0$ correspond to the occurrence of QZE and QAZE in i th mode. Clearly, the negative (positive) values of the Zeno parameter represent that the number of photon/phonons in the system waveguide (i.e., $\langle N_i \rangle$) decreases (increases) from that in the absence of the probe waveguide (i.e., $\langle N_i \rangle_{\Gamma=0}$). We have reported the dynamics of number operators for Stokes, anti-Stokes, and phonon modes in Appendix A. In what follows, we report the Zeno parameters for Stokes, anti-Stokes, and phonon modes obtained using these expressions.

To begin with, using Eq. (A2) in Eq. (4), the Zeno parameter for the Stokes mode is computed as

$$Z_b = \mathcal{C}_b \left\{ \frac{\cos \theta_2}{\Delta\omega_S(\Delta\omega_D + \Delta\omega_S)} + \frac{\cos(\Delta\omega_S z + \Delta\omega_D z - \theta_2)}{\Delta\omega_D(\Delta\omega_D + \Delta\omega_S)} - \frac{\cos(\Delta\omega_S z - \theta_2)}{\Delta\omega_D \Delta\omega_S} \right\}, \quad (5)$$

where we have used phase mismatches with probe–Stokes and probe–anti-Stokes process as $\theta_1 = (\varphi_d - \varphi_p - \varphi_c)$ and $\theta_2 = (\varphi_p - \varphi_b - \varphi_c)$, respectively. Also, we have $\mathcal{C}_b =$

$2\Gamma g \left(|\alpha_1|^2 + |\alpha_2|^2 + 1 \right) |\alpha| |\beta| |\gamma|$. Similarly, we have introduced frequency detuning parameters in Stokes, anti-Stokes, and second-order coupling between the probe and system waveguides as $\Delta\omega_S = -\omega_{a_1} - \omega_{a_2} + \omega_b + \omega_c$, $\Delta\omega_A = \omega_{a_1} + \omega_{a_2} + \omega_c - \omega_d$, and $\Delta\omega_D = \omega_{a_1} + \omega_{a_2} - \omega_p$.

In the similar manner, the Zeno parameter for the anti-Stokes mode is computed using Eqs. (4) and (A4) and the following analytic expression is obtained

$$Z_d = \mathcal{C}_d \left\{ \frac{\cos \theta_1}{\Delta\omega_A(\Delta\omega_A - \Delta\omega_D)} - \frac{\cos(\theta_1 + \Delta\omega_D z - \Delta\omega_A z)}{\Delta\omega_D(\Delta\omega_A - \Delta\omega_D)} + \frac{\cos(\theta_1 - \Delta\omega_A z)}{\Delta\omega_D \Delta\omega_A} \right\}, \quad (6)$$

where $\mathcal{C}_d = 2\Gamma\chi \left(|\alpha_1|^2 + |\alpha_2|^2 + 1 \right) |\alpha| |\gamma| |\delta|$. Zeno parameter for the phonon mode was also computed analytically using Eqs. (4)-(A3), but it was found that the same can be expressed as the difference of the other two Zeno parameters, i.e.,

$$Z_c = Z_b - Z_d. \quad (7)$$

This is a direct consequence of the conservation law: $[G, N_c + N_d - N_b] = 0$, and thus using this constant of motion [37] Eq. (7) follows. Apparently, this should be the case with degenerate hyper-Raman and Raman processes in the system, too, provided the probe-system interaction is with the pump mode, however, the probe-system interaction may be with the Stokes and anti-Stokes modes as in the case of earlier works [10].

IV. DISCUSSION

There are some interesting scenarios to consider for the present study, namely spontaneous, stimulated, and partially stimulated cases. Specifically, from the expressions of \mathcal{C}_j , we can easily observe that in the spontaneous case, when $\alpha_i \neq 0$, $\alpha \neq 0$ and $\beta = \gamma = \delta = 0$, $Z_j = 0 \forall j \in \{b, c, d\}$. Thus, neither QZE nor QAZE is observed in the spontaneous case. The stimulated case, i.e., when all coherent modes are initially

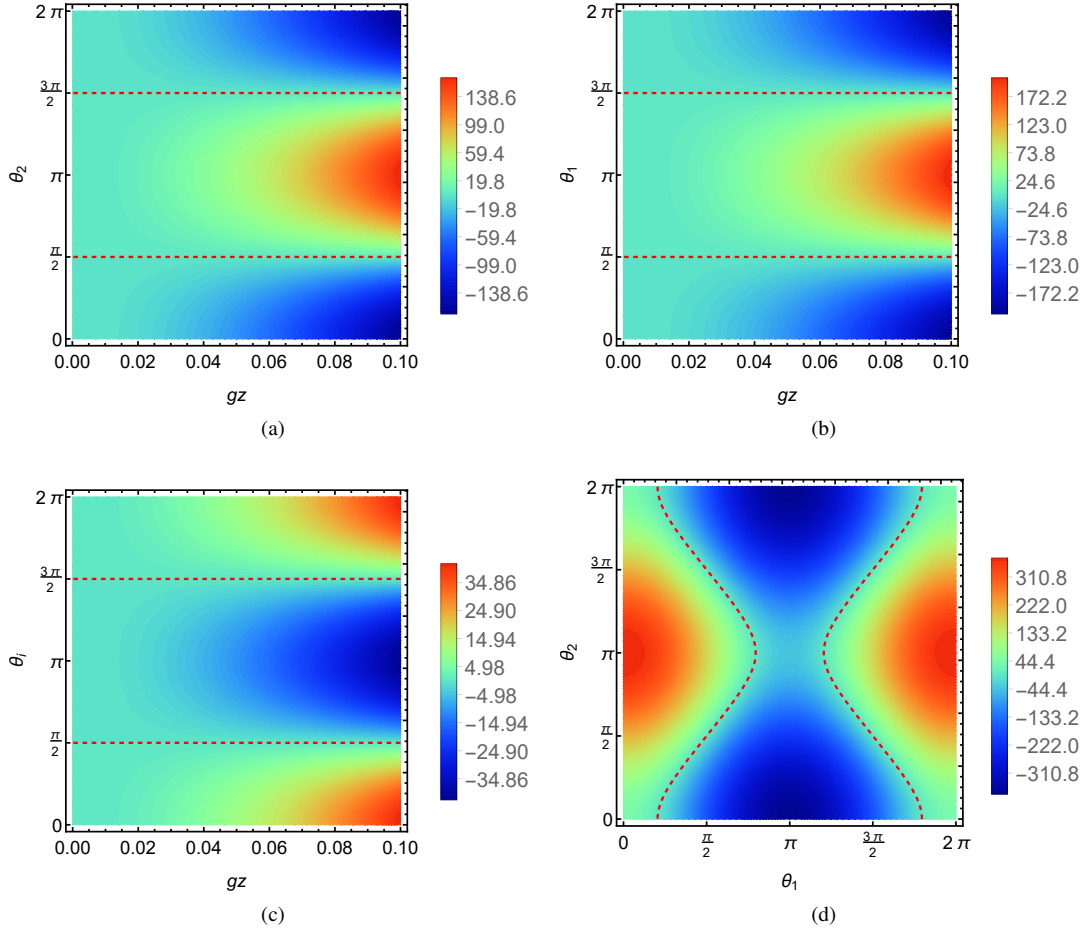


Figure 2. (Color online) Spatial evolution of Zeno parameter Z_j for (a) Stokes, (b) anti-Stokes, and (c)-(d) phonon modes as a function of the phase mismatch parameter θ_i . In (c), we have shown Z_c ($\theta_1 = \theta_2$). We have chosen here coupling coefficients $\chi = 10g$, $\Gamma = 100g$ with initial coherent state amplitudes for all modes $\alpha = 11, \alpha_1 = 10, \alpha_2 = 9.5, \beta = 8, \gamma = 0.01, \delta = 1$. We have also used $\Delta\omega_S = \Delta\omega_A = 10^{-2}g = 10\Delta\omega_D$. The dashed (red) contour lines represent a crossover between QZE and QAZE. All the quantities shown here and the rest of the plots are dimensionless.

prepared with non-zero intensity, will be discussed in detail later. Prior to that, we may discuss the partially stimulated cases, where among Stokes, anti-Stokes and phonon modes, initial intensity is nonzero for at most two modes and the same for other modes(s) is zero; of course the pump modes have nonzero initial intensity. Consider a particular type of stimulated case, where $\alpha_i \neq 0, \alpha \neq 0$ and $\beta \neq 0, \gamma \neq 0, \delta = 0$. In this case, we obtain $Z_d = 0 \neq Z_b = Z_c$; while with $\alpha_i \neq 0, \alpha \neq 0$ and $\beta = 0, \gamma \neq 0, \delta \neq 0$ we obtain $Z_d = -Z_c \neq 0 = Z_b$. Thus, in the first type of partially stimulated case mentioned above, for a particular choice of phase mismatching and frequency detuning parameters, if we observe QZE (QAZE) in Stokes mode, we will observe QZE (QAZE) in phonon mode, too, but the anti-Stokes mode will not show any of the effects. Similarly, in the second type of partially stimulated case, for a particular choice of phase mismatching and frequency detuning parameters, if we observe QZE (QAZE) in anti-Stokes mode, we will observe QAZE (QZE) in phonon mode, Stokes mode will not show any of the

effects. The other possibility of partially stimulated process with $\alpha_i \neq 0, \alpha \neq 0$ and $\beta \neq 0, \gamma = 0, \delta \neq 0$ leads to a trivial case where $Z_j = 0$ as $\mathcal{C}_j \propto |\gamma| \forall j \in \{b, c, d\}$. There are a couple of other possibilities where two of the parameters α, β, γ are simultaneously zero. It is easy to see that neither QZE nor QAZE will be observed in those cases. Specifically, for $\beta = 0, \gamma = 0, \delta \neq 0$ and $\beta \neq 0, \gamma = 0, \delta = 0$, we would not obtain QZE or QAZE in any mode as $\gamma = 0$ would ensure that $Z_j = 0 \forall j \in \{b, c, d\}$. The same situation will arise in the case $\beta = 0, \gamma \neq 0, \delta = 0$ as \mathcal{C}_j will vanish $\forall j \in \{b, c, d\}$.

From Eqs. (5)-(6), we can verify that $\mathcal{C}_j \propto 2\Gamma \left(|\alpha_1|^2 + |\alpha_2|^2 + 1 \right) |\alpha| |\gamma| \forall j \in \{b, c, d\}$ which is always positive and increases with coupling between the probe and system as well as initial pump and probe intensities and phonon numbers. Additionally, we can verify that $\mathcal{C}_b \propto g|\beta|$ and $\mathcal{C}_d \propto \chi|\delta|$. Thus, we can conclude that the coefficients \mathcal{C}_j can only alter the depth of Zeno parameters by a scaling factor, but cannot induce a transition from QZE to QAZE or vice-versa. Therefore, we can summarize that the occurrence

of QZE or QAZE would depend only on the detuning parameters and phase mismatches, i.e., we can safely restrict our discussion on the possibility of observing QZE and QAZE to a situation where the parametric dependence of the relevant Zeno parameters is viewed as $Z_b(\Delta\omega_D, \Delta\omega_S, \theta_2)$ and $Z_d(\Delta\omega_D, \Delta\omega_A, \theta_1)$. This analytic result helps us to clearly visualize the interplay between QZE and QAZE, and it also answers: What controls the dynamics of QZE and QAZE and which physical parameters may cause transition from one of them to the other? Before we discuss it further, it is worth discussing the behavior for resonant hyper-Raman system waveguide.

Considering the resonant condition that $\Delta\omega_D = \Delta\omega_S = \Delta\omega_A = 0$ we can obtain from Eqs. (5)-(7), in the limits of frequency detunings tending to zero, that

$$(Z_b)_R = -\frac{1}{2}C_b z^2 \cos \theta_2 \quad (8)$$

and

$$(Z_d)_R = -\frac{1}{2}C_d z^2 \cos \theta_1, \quad (9)$$

where R corresponds to the resonant condition. Notice that phase difference parameters are significant in the presence of QZE and QAZE as $(Z_j)_R \propto -\cos \theta_i$, while the depth of the Zeno parameters increases with C_j and propagation length z . We know that $\cos \theta_i > 0 \forall \theta_i \in \{[0, \frac{\pi}{2}] \cup [\frac{3\pi}{2}, 2\pi]\}$ and $\cos \theta_i < 0 \forall \theta_i \in \{[\frac{\pi}{2}, \frac{3\pi}{2}]\}$. Thus, QAZE (QZE) is observed in both Stokes and anti-Stokes modes when $\cos \theta_i$ is negative (positive). In this case, $(Z_c)_R = -(C_b \cos \theta_2 - C_d \cos \theta_1) z^2$, which has dependence on both phase difference parameters. If we consider $\theta_1 = \theta_2$, this will reduce to $(Z_c)_R|_{\theta_1=\theta_2} = -(C_b - C_d) z^2 \cos \theta_i$, and thus, in this special case, QZE (QAZE) would be observed in phonon mode if $\frac{g}{\chi} > \frac{|\delta|}{|\beta|}$ ($\frac{g}{\chi} < \frac{|\delta|}{|\beta|}$). Interestingly, most of the observations made here regarding phase mismatch parameters are also applicable in off-resonant hyper-Raman case with small frequency detunings (cf. Fig. 2).

Consider a special case of off-resonant hyper-Raman process in the system waveguide, when $\Delta\omega_D = \Delta\omega_S = -\Delta\omega_A$ corresponding to phonon excitation. Here, $\Delta\omega_S = -\Delta\omega_A$ ensures the phonon excitation as $2\omega_c = \omega_d - \omega_b$. In this case, Eqs. (5)-(7) can be simplified to obtain

$$Z_j = -\frac{1}{2}C_j z^2 \cos(\Delta\omega_D z + (-1)^i \theta_i) \text{sinc}^2\left(\frac{\Delta\omega_D z}{2}\right), \quad (10)$$

where $i = 1$ for $j = d$ and $i = 2$ for $j = b$. It clearly shows that the general solution used here is modulated with sinc function of the frequency detuning parameter [38, 39]. Consequently, the present solution and corresponding results are applicable to a relatively long length of the optical coupler in comparison to the corresponding short-length solution. Notice in Eq. (10) that $Z_j \propto \cos(\Delta\omega_D z + (-1)^j \theta_i)$, and thus a crossover between QZE and QAZE can be attained by controlling the frequency detuning $\Delta\omega_D$. Therefore, if we assume phase mismatch parameter $\theta_i = 0$, we can conclude that Z_j is negative (i.e., QZE is observed) only when $\Delta\omega_D z \in \{[0, \frac{\pi}{2}] \cup [\frac{3\pi}{2}, 2\pi]\}$, otherwise QAZE is observed.

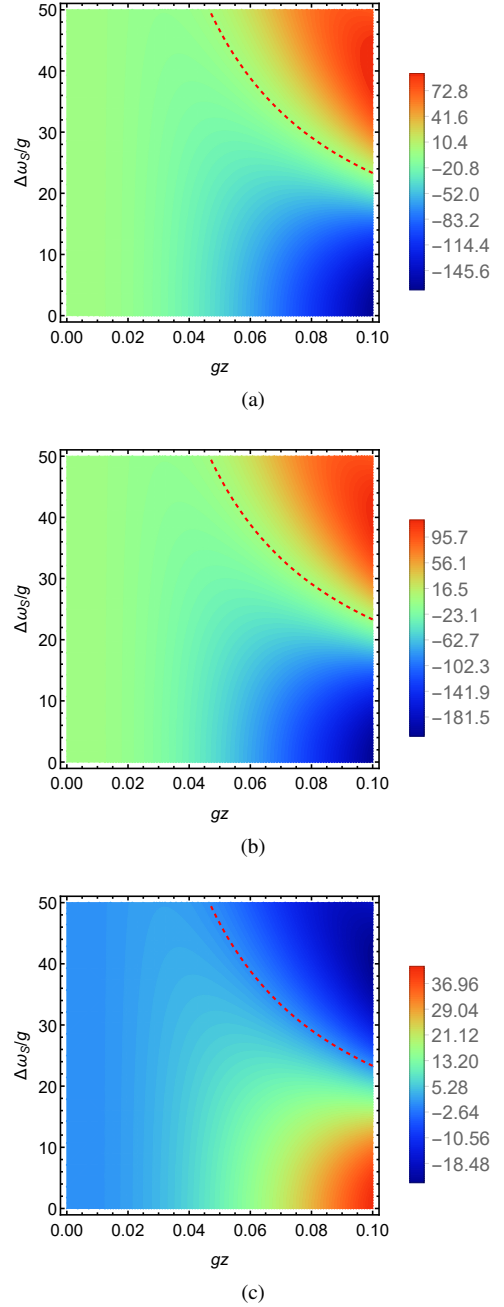


Figure 3. (Color online) Spatial evolution of Zeno parameter Z_j as a function of frequency detuning parameter for (a) Stokes, (b) anti-Stokes, and (c) phonon modes considering both phase mismatch parameters $\theta_i = 0$ with $\Delta\omega_D = 10^{-3}g$ and $\Delta\omega_A = \Delta\omega_S$. The rest of the parameters are same as in the previous figure.

To further stress on this point, we have shown variation of the Zeno parameters with frequency detuning parameters in Fig. 3, where we can clearly see that a transition from QZE (QAZE) to QAZE (QZE) can be caused in both optical modes (phonon mode) for large values of frequency detuning after traversing sufficiently through the optical coupler. In all the plots, we have considered $\Delta\omega_S = \Delta\omega_A$ (unless stated otherwise) corresponding to the conservation of radiation energy as

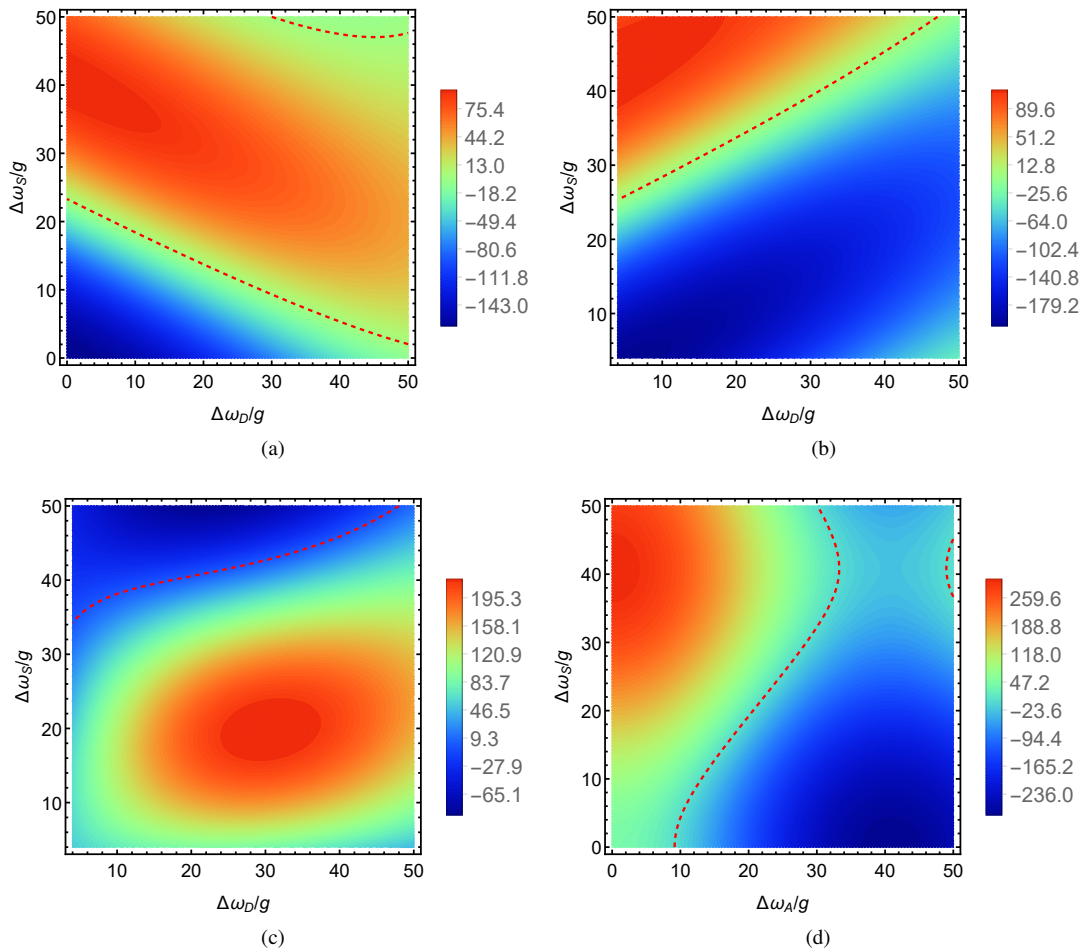


Figure 4. (Color online) Variation of Zeno parameters as a function of frequency detuning parameters for (a) Stokes Z_b ($\Delta\omega_S, \Delta\omega_D$), (b) anti-Stokes Z_d ($\Delta\omega_A = \Delta\omega_S, \Delta\omega_D$), (c) phonon Z_c ($\Delta\omega_A = \Delta\omega_S, \Delta\omega_D$), and (d) phonon Z_c ($\Delta\omega_S, \Delta\omega_A, \Delta\omega_D = 10^{-3}g$) modes considering both phase mismatch parameters $\theta_i = 0$ and $gz = 0.1$. The rest of the parameters are same as the previous figure.

$$2(\omega_{a_1} + \omega_{a_2}) = \omega_b + \omega_d.$$

Taking into consideration both frequency detuning parameters together (considering there is no phase mismatch), a transition from QZE to QAZE in Stokes mode can be induced for smaller values of the detuning parameter than that shown in Fig. 3 (a) by increasing the other detuning parameter (shown in Fig. 4 (a)). In contrast, QZE for anti-Stokes mode can be maintained for larger values of frequency detuning in anti-Stokes generation by increasing the value of frequency detuning between the pump modes of the system and probe waveguides (cf. Figs. 3 (b) and 4 (b)). Similarly, QAZE can be made more dominant by increasing frequency detuning between the pump modes of the system and probe as shown in Fig. 4 (c). Interestingly, frequency detuning in Stokes and anti-Stokes generation processes have starkly opposite effects on the Zeno parameter as the former increases it while the latter decreases it (cf. Fig. 4 (d)).

Further extension of the present results with phonon mode initially coherent to the chaotic phonon mode [38] gives that all the Zeno parameters become zero. Our results can also be used to deduce the presence of QZE and QAZE for degenerate

hyper-Raman and Raman system waveguides from Eqs. (5)-(7) by considering $\alpha_2 = \alpha_1$ and $\alpha_2 = 0$, respectively. Therefore, we can conclude from the reduced results in those cases that the presence of QZE and QAZE in the parametric space will remain unchanged, though some changes in the depth of the Zeno parameter is expected due to changes in the scaling factors C_j .

V. CONCLUSION

The dynamics of a nonlinear waveguide operating under hyper-Raman process is obtained in terms of the spatial evolution of the photon and phonon numbers of the Stokes, anti-Stokes, and vibration modes. We subsequently consider that this waveguide (referred to as a system) is constantly gazed upon by a probe waveguide interacting with the non-degenerate pump modes of the hyper-Raman process. We obtain the dynamics of the system waveguide in this combined system-probe optical coupler in a completely quantum treatment by solving the Heisenberg's equations of motion for the

corresponding momentum operator. These two cases allow us to quantify the effect of the presence of the probe waveguide on the system waveguide as Zeno parameter. Specifically, if the presence of the probe is found to enhance (suppress) the generation of bosons in Stokes, anti-Stokes, and phonon modes it is referred to as QAZE (QZE).

The conservation of Stokes–anti-Stokes photon and phonon numbers is reflected in the relation between the Zeno parameters for the concerned modes. To be specific, the Zeno parameter for the phonon mode is the difference between that of the Stokes and anti-Stokes modes. The present study allows us to conclude that both QZE and QAZE disappear in spontaneous and some of the partially stimulated cases. Interestingly, the Zeno parameter depends on the intensities of pump, probe, and phonon modes as well as the system-probe coupling strength. However, none of these parameters can cause a crossover from QZE to QAZE and vice versa, as they always remain positive and thus can only alter the depth of the Zeno parameter. A similar effect was shown by the spatial evolution for the small values of frequency detuning parameters.

Interestingly, the hyper-Raman based optical coupler both at resonance and off-resonance shown dependence on phase mismatch parameters in Stokes and anti-Stokes generation processes. Similarly, the frequency detuning parameters offer another set of control parameters to induce a transition between QZE and QAZE. In short, we have analytically ob-

tained solution of an interesting question: Which physical parameters controls the dynamics of QZE and QAZE and which of them can cause a transition from QZE to QAZE and vice versa.

Due to a general nature of the system under consideration, namely non-degenerate hyper-Raman process, the obtained results can be reduced to corresponding Raman and degenerate hyper-Raman processes. Specifically, the dependence on all the parameters and the nature of the Zeno parameter in these special cases is expected to be similar to the present case with only a scaling factor. We conclude the present work in hope that this work focused on foundationally relevant topic will lead to applications in counterfactual quantum communication and computation as the physical system considered here and all its special cases are physically realizable using current technologies available in the domain of integrated optics as well as conventional bulk optics.

Acknowledgments: AP acknowledges the support from Interdisciplinary Cyber Physical Systems (ICPS) programme of the Department of Science and Technology (DST), India, Grant No.: DST/ICPS/QuST/Theme-1/2019/14. KT acknowledges the financial support from the Operational Programme Research, Development and Education - European Regional Development Fund project no. CZ.02.1.01/0.0/0.0/16_019/0000754 of the Ministry of Education, Youth and Sports of the Czech Republic.

-
- [1] B. Misra and E. C. G. Sudarshan, *J. Math. Phys.* **18**, 756-763 (1977).
- [2] L. A. Khalifin, *Dokl. Akad. Nauk SSSR* **115**, 277 (1957) [*Sov. Phys. Dokl.* **2**, 232 (1958)]; *Zh. Eksp. Teor. Fiz.* **33**, 1371 (1958) [*Sov. Phys. JETP* **6**, 1053 (1958)]; *Dokl. Akad. Nauk SSSR* **141**, 599 (1961) [*Sov. Phys. Dokl.* **6**, 1010 (1962)]
- [3] A. Venugopalan, *Resonance* **12**, 52 (2007).
- [4] P. Facchi and S. Pascazio, in *Quantum Zeno and Inverse Quantum Zeno Effects*, edited by E. Wolf, *Progress in Optics* Vol. 42 (Elsevier, Amsterdam, 2001), pp. 147-218.
- [5] S. Pascazio, *Open Systems and Information Dynamics* **21**, 1440007 (2014).
- [6] K. Thapliyal and A. Pathak, *Proceedings of International Conference on Optics and Photonics, February 20-22, Kolkata, India*, *Proc. of SPIE* **9654**, 96541F1 (2015).
- [7] J. Naikoo, K. Thapliyal, S. Banerjee, and A. Pathak, *Phys. Rev. A* **99**, 023820 (2019).
- [8] K. Thapliyal, A. Pathak, and J. Peřina, *Phys. Rev. A* **93**, 022107 (2016).
- [9] P. Facchi, and S. Pascazio, Three different manifestations of the quantum Zeno effect. *Lecture notes in Physics* **622**, 141 (2003).
- [10] K. Thun, J. Peřina, and J. Křepelka, *Phys. Lett. A* **299**, 19 (2002).
- [11] J. Řeháček, J. Peřina, P. Facchi, S. Pascazio, and L. Miřta Jr, *Opt. Spectrosc.* **91**, 501 (2001).
- [12] L. Miřta Jr, V. Jelínek, J. Řeháček, and J. Peřina, *J. Opt. B: Quantum Semiclassical Opt.* **2**, 726 (2000).
- [13] J. Řeháček, J. Peřina, P. Facchi, S. Pascazio, and L. Miřta, *Phys. Rev. A* **62**, 013804 (2000).
- [14] A. Luis and J. Peřina, *Phys. Rev. Lett.* **76**, 4340 (1996).
- [15] A. Luis and L. L. Sánchez-Soto, *Phys. Rev. A* **57**, 781 (1998).
- [16] J. Řeháček, J. Peřina, P. Facchi, S. Pascazio, and L. Miřta, *Phys. Rev. A* **62**, 013804 (2000).
- [17] J. Peřina, *Phys. Lett. A* **325**, 16 (2004).
- [18] G. S. Agarwal and S. P. Tewari, *Phys. Lett. A* **185**, 139 (1994).
- [19] P. G. Kwiat, A. G. White, J. R. Mitchell, O. Nairz, G. Weihs, H. Weinfurter, and A. Zeilinger, *Phys. Rev. Lett.* **83**, 4725 (1999).
- [20] W. M. Itano, D. J. Heinzen, J. J. Bollinger, and D. J. Wineland, *Phys. Rev. A* **41**, 2295 (1990).
- [21] M. C. Fischer, B. Gutiérrez-Medina, and M. G. Raizen, *Phys. Rev. Lett.* **87**, 040402 (2001).
- [22] O. Hosten, M. T. Rakher, J. T. Barreiro, N. A. Peters, and P. G. Kwiat, *Nature* **439**, 949 (2006).
- [23] H. Salih, Z. H. Li, M. Al-Amri, and M. S. Zubairy, *Phys. Rev. Lett.* **110**, 170502 (2013).
- [24] P. Facchi, Z. Hradil, G. Krenn, S. Pascazio, and J. Řeháček, *Phys. Rev. A* **66**, 012110 (2002).
- [25] S. Pascazio, P. Facchi, Z. Hradil, G. Krenn, and J. Řeháček, *Fortschritte der Physik* **49**, 1071 (2001).
- [26] A. Tavakoli, H. Anwer, A. Hameedi, and M. Bourennane, *Phys. Rev. A* **92**, 012303 (2015).
- [27] A. Beige, D. Braun, B. Tregenna, and P. L. Knight, *Phys. Rev. Lett.* **85**, 1762 (2000).
- [28] Y. Cao, Y.-H. Li, Z. Cao, J. Yin, Y.-A. Chen, H.-L. Yin, T.-Y. Chen, X. Ma, C.-Z. Peng, and J.-W. Pan, *Proc. of the Nat. Acad. Sci.* **114**, 4920 (2017).
- [29] H. Nikolić, *Phys. Lett. B* **733**, 6 (2014).
- [30] D. A. Zezyulin, V. V. Konotop, G. Barontini, and H. Ott, *Phys. Rev. Lett.* **109**, 020405 (2012).
- [31] J. L. O'brien, A. Furusawa, and J. Vučković, *Nature Photonics* **3**, 687 (2009).
- [32] A. Politi, M. J. Cryan, J. G. Rarity, S. Yu, and J. L. O'brien,

Science **320**, 646 (2008).

- [33] K. Thapliyal, A. Pathak, B. Sen, and J. Peřina, Phys. Rev. A **90**, 013808 (2014).
 [34] K. Thapliyal, A. Pathak, B. Sen, and J. Peřina, Phys. Lett. A **378**, 3431-3440 (2014).
 [35] B. Sen and S. Mandal, J. Mod. Opt. **52**, 1789 (2005).
 [36] S. Mandal and J. Peřina, Phys. Lett. A **328**, 144 (2004).
 [37] J. Peřina, Quantum Statistics of Linear and Nonlinear Optical Phenomena, Kluwer Academic, Dordrecht-Boston (1991).
 [38] K. Thapliyal and J. Peřina, Phys. Lett. A **383**, 2011 (2019).
 [39] K. Thapliyal and J. Peřina, Phys. Scr. **95**, 034001 (2020).

Appendix A: Mathematical details of the solution

The Heisenberg's equations of motion for all six modes in the probe and system waveguides can be obtained as

$$\begin{aligned}
 \dot{a}_p(z) &= i(\omega_p a_p + \Gamma a_1 a_2), \\
 \dot{a}_1(z) &= i\left(\omega_{a_1} a_1 + g a_2^\dagger b c + \chi a_2^\dagger c^\dagger d + \Gamma a_p a_2^\dagger\right), \\
 \dot{a}_2(z) &= i\left(\omega_{a_2} a_2 + g a_1^\dagger b c + \chi a_1^\dagger c^\dagger d + \Gamma a_p a_1^\dagger\right), \\
 \dot{b}(z) &= i(\omega_b b + g a_1 a_2 c^\dagger), \\
 \dot{c}(z) &= i\left(\omega_c c + g a_1 a_2 b^\dagger + \chi a_1^\dagger a_2^\dagger d\right), \\
 \dot{d}(z) &= i(\omega_d d + \chi a_1 a_2 c).
 \end{aligned} \tag{A1}$$

This set of coupled operator differential equations is not exactly solvable in the closed analytic form. A perturbative solution of the coupled differential equations (A1) is obtained up to the quadratic terms in the interaction constants (g, χ , and Γ). Using the obtained spatial evolution of all the field and phonon modes in the closed analytic form, we obtained the number operators for Stokes, phonon, and anti-Stokes modes as

$$\begin{aligned}
 \langle N_b \rangle &= |\beta|^2 + |j_2|^2 |\alpha_1|^2 |\alpha_2|^2 (|\gamma|^2 + 1) + \{j_1 j_2^* \alpha_1^* \alpha_2^* \\
 &\times \beta \gamma + j_1 j_3^* \alpha_1^{*2} \alpha_2^{*2} \beta \delta + j_1 j_4^* (|\alpha_1|^2 + 1) \beta \gamma^2 \delta^* \\
 &+ j_1 j_5^* |\alpha_2|^2 \beta \gamma^2 \delta^* + j_1 j_6^* (|\alpha_1|^2 + 1) \alpha^* \beta \gamma \\
 &+ j_1 j_7^* |\alpha_2|^2 \alpha^* \beta \gamma + j_1 j_8^* |\alpha_1|^2 |\alpha_2|^2 |\beta|^2 + j_1 j_9^* |\beta|^2 \\
 &\times (|\alpha_1|^2 + 1) |\gamma|^2 + j_1 j_{10}^* |\alpha_2|^2 |\beta|^2 |\gamma|^2 + \text{c.c.}\}, \tag{A2}
 \end{aligned}$$

$$\begin{aligned}
 \langle N_c \rangle &= |\gamma|^2 + |k_2|^2 |\alpha_1|^2 |\alpha_2|^2 (|\beta|^2 + 1) + |k_3|^2 \\
 &\times (|\alpha_1|^2 + 1) (|\alpha_2|^2 + 1) |\delta|^2 + \{k_1 k_2^* \alpha_1^* \alpha_2^* \beta \gamma \\
 &+ k_1 k_3^* \alpha_1 \alpha_2 \gamma \delta^* + k_1 k_4^* (|\alpha_1|^2 + 1) \alpha^* \beta \gamma \\
 &+ k_1 k_5^* |\alpha_2|^2 \alpha^* \beta \gamma + k_1 k_6^* |\alpha_1|^2 \alpha \gamma \delta^* \\
 &+ k_1 k_7^* (|\alpha_2|^2 + 1) \alpha \gamma \delta^* + k_2 k_3^* \alpha_1^2 \alpha_2^2 \beta^* \delta^* \\
 &+ k_1 k_8^* |\alpha_1|^2 |\alpha_2|^2 |\gamma|^2 + k_1 k_9^* (|\alpha_1|^2 + 1) \\
 &\times |\beta|^2 |\gamma|^2 + k_1 k_{10}^* |\alpha_2|^2 |\beta|^2 |\gamma|^2 + k_1 k_{11}^* |\alpha_1|^2 \\
 &\times |\gamma|^2 |\delta|^2 + k_1 k_{12}^* (|\alpha_2|^2 + 1) |\gamma|^2 |\delta|^2 \\
 &+ k_1 k_{13}^* |\alpha_1|^2 |\alpha_2|^2 |\gamma|^2\} + \text{c.c.}, \tag{A3}
 \end{aligned}$$

and

$$\begin{aligned}
 \langle N_d \rangle &= |\delta|^2 + |l_2|^2 |\alpha_1|^2 |\alpha_2|^2 |\gamma|^2 + \{l_1 l_2^* \alpha_1^* \alpha_2^* \gamma^* \delta \\
 &+ l_1 l_3^* (|\alpha_1|^2 + 1) \beta^* \gamma^* \delta + l_1 l_4^* |\alpha_2|^2 \beta^* \gamma^* \delta \\
 &+ l_1 l_5^* \alpha_1^{*2} \alpha_2^{*2} \beta \delta + l_1 l_6^* (|\alpha_1|^2 + 1) \alpha^* \gamma^* \delta \\
 &+ l_1 l_7^* |\alpha_2|^2 \alpha^* \gamma^* \delta + l_1 l_8^* (|\alpha_1|^2 + 1) |\gamma|^2 |\delta|^2 \\
 &+ l_1 l_9^* |\alpha_2|^2 |\gamma|^2 |\delta|^2 + l_1 l_{10}^* (|\alpha_1|^2 + 1) \\
 &\times (|\alpha_2|^2 + 1) |\delta|^2\} + \text{c.c.}, \tag{A4}
 \end{aligned}$$

respectively. The functional form of coefficients of complex amplitude parameters are

$$\begin{aligned}
 \frac{j_1}{j_1} &= e^{iz\omega_b}, \\
 \frac{j_2}{j_1} &= \frac{g(1 - e^{-iz\Delta\omega_S})}{\Delta\omega_S}, \\
 \frac{j_3}{j_1} &= \frac{g\chi(\Delta\omega_A - \Delta\omega_1 e^{-iz\Delta\omega_S} - \Delta\omega_S e^{iz\Delta\omega_1})}{\Delta\omega_A \Delta\omega_1 \Delta\omega_S}, \\
 \frac{j_4}{j_1} &= \frac{j_5}{j_1} = \frac{g\chi(\Delta\omega_A + \Delta\omega_S e^{-iz\Delta\omega_2} - \Delta\omega_2 e^{-iz\Delta\omega_S})}{\Delta\omega_A \Delta\omega_S \Delta\omega_2}, \\
 \frac{j_6}{j_1} &= \frac{j_7}{j_1} = \frac{g\Gamma(\Delta\omega_D + \Delta\omega_S e^{-iz\Delta\omega_3} - \Delta\omega_3 e^{-iz\Delta\omega_S})}{\Delta\omega_D \Delta\omega_S \Delta\omega_3}, \\
 \frac{j_8}{j_1} &= -\frac{j_9}{j_1} = -\frac{j_{10}}{j_1} = \frac{g^2(1 - e^{-iz\Delta\omega_S} - i\Delta\omega_S z)}{\Delta\omega_S^2},
 \end{aligned} \tag{A5}$$

$$\begin{aligned}
 \frac{k_1}{k_1} &= e^{iz\omega_c}, \\
 \frac{k_2}{k_1} &= \frac{g(1 - e^{-iz\Delta\omega_S})}{\Delta\omega_S}, \\
 \frac{k_3}{k_1} &= \frac{\chi(1 - e^{-iz\Delta\omega_A})}{\Delta\omega_A}, \\
 \frac{k_4}{k_1} &= \frac{k_5}{k_1} = \frac{g\Gamma(\Delta\omega_D + \Delta\omega_S e^{-iz\Delta\omega_3} - \Delta\omega_3 e^{-iz\Delta\omega_S})}{\Delta\omega_D \Delta\omega_S \Delta\omega_3}, \\
 \frac{k_6}{k_1} &= \frac{k_7}{k_1} = \frac{\Gamma\chi(-\Delta\omega_D + \Delta\omega_A e^{iz\Delta\omega_4} - \Delta\omega_4 e^{-iz\Delta\omega_A})}{\Delta\omega_A \Delta\omega_D \Delta\omega_4}, \\
 \frac{k_8}{k_1} &= -\frac{k_{11}}{k_1} = -\frac{k_{12}}{k_1} = -\frac{\chi^2(1 - e^{-iz\Delta\omega_A} - i\Delta\omega_A z)}{\Delta\omega_A^2}, \\
 \frac{k_9}{k_1} &= \frac{k_{10}}{k_1} = -\frac{k_{13}}{k_1} = -\frac{g^2(1 - e^{iz\Delta\omega_S} - i\Delta\omega_S z)}{\Delta\omega_S^2},
 \end{aligned} \tag{A6}$$

and

$$\begin{aligned}
 \frac{l_1}{l_1} &= e^{iz\omega_d}, \\
 \frac{l_2}{l_1} &= -\frac{\chi(1 - e^{iz\Delta\omega_A})}{\Delta\omega_A}, \\
 \frac{l_3}{l_1} &= \frac{l_4}{l_1} = \frac{g\chi(\Delta\omega_S + \Delta\omega_A e^{iz\Delta\omega_2} - \Delta\omega_2 e^{iz\Delta\omega_A})}{\Delta\omega_S \Delta\omega_A \Delta\omega_2}, \\
 \frac{l_5}{l_1} &= \frac{l_6}{l_1} = \frac{g\chi(\Delta\omega_S + \Delta\omega_1 e^{iz\Delta\omega_A} - \Delta\omega_A e^{iz\Delta\omega_1})}{\Delta\omega_S \Delta\omega_1 \Delta\omega_A}, \\
 \frac{l_7}{l_1} &= \frac{l_8}{l_1} = \frac{\Gamma\chi(\Delta\omega_D - \Delta\omega_A e^{iz\Delta\omega_4} + \Delta\omega_4 e^{iz\Delta\omega_A})}{\Delta\omega_D \Delta\omega_A \Delta\omega_4}, \\
 \frac{l_9}{l_1} &= \frac{l_{10}}{l_1} = -\frac{l_{11}}{l_1} = -\frac{\chi^2(1 - e^{iz\Delta\omega_A} + i\Delta\omega_A z)}{\Delta\omega_A^2},
 \end{aligned} \tag{A7}$$

where $\Delta\omega_1 = (2\omega_{a_1} + 2\omega_{a_2} - \omega_b - \omega_d)$, $\Delta\omega_2 = (\omega_b + 2\omega_c - \omega_d)$, $\Delta\omega_3 = (\omega_b + \omega_c - \omega_p)$, $\Delta\omega_4 = (\omega_c - \omega_d + \omega_p)$, $\Delta\omega_S = (-\omega_{a_1} - \omega_{a_2} + \omega_b + \omega_c)$, $\Delta\omega_A = (\omega_{a_1} + \omega_{a_2} + \omega_c - \omega_d)$, and $\Delta\omega_D = (\omega_{a_1} + \omega_{a_2} - \omega_p)$.